SUPPLEMENTAL REPORT

OPTIMIZED DEPOSITION PARAMETERS & COATING PROPERTIES OF COBALT PHOSPHORUS ALLOY ELECTROPLATING FOR TECHNOLOGY INSERTION RISK REDUCTION

(ESTCP Project WP-0411)

Ruben Prado & John Benfer
Naval Air Systems Command

Diana Facchini
Integran Technologies, Inc.

Keith Legg
Rowan Technology Group

October 2010
Final Version

Report Documentation Page

Form Approved
OMB No. 0704-0188

1. REPORT DATE	2. REPORT TYPE	3. DATES COVERED
OCT 2010	**N/A**	**-**

4. TITLE AND SUBTITLE	5a. CONTRACT NUMBER
Optimized Deposition Parameters & Coating Properties of Cobalt Phosphorus Alloy Electroplating for Technology Insertion Risk Reduction	5b. GRANT NUMBER
	5c. PROGRAM ELEMENT NUMBER
6. AUTHOR(S)	5d. PROJECT NUMBER
	5e. TASK NUMBER
	5f. WORK UNIT NUMBER
7. PERFORMING ORGANIZATION NAME(S) AND ADDRESS(ES) **NAVAIR ISSC/FRC-SE NAS Jacksonville Bldg 793, Code 434 Jacksonville, FL 32212**	8. PERFORMING ORGANIZATION REPORT NUMBER
9. SPONSORING/MONITORING AGENCY NAME(S) AND ADDRESS(ES)	10. SPONSOR/MONITOR'S ACRONYM(S)
	11. SPONSOR/MONITOR'S REPORT NUMBER(S)

12. DISTRIBUTION/AVAILABILITY STATEMENT
Approved for public release, distribution unlimited

13. SUPPLEMENTARY NOTES
ESTCP Project WP-0411 Supplemental Report, The original document contains color images.

14. ABSTRACT
Optimized plating deposition parameters were obtained using a Design of Experiment (DOE) approach. These parameters were validated through supplemental testing and found to be non-embrittling with improved fatigue and neutral salt fog corrosion performance as compared to hard chromium electroplate. The nCoP deposit did exhibit reduced hardness (560 VHN) and reduced taber wear abrasion performance as compared to hard chromium electroplate. Producibility evaluations were performed utilizing a J52 Shaft section and a J52 Coupling component. Optimized plating parameters were successfully demonstrated on both ID & OD areas. The above plated components were then finished machined at FRC-SE with no observable defects.

15. SUBJECT TERMS

16. SECURITY CLASSIFICATION OF:			17. LIMITATION OF ABSTRACT	18. NUMBER OF PAGES	19a. NAME OF RESPONSIBLE PERSON
a. REPORT	b. ABSTRACT	c. THIS PAGE			
unclassified	**unclassified**	**unclassified**	**SAR**	**50**	

REPORT DOCUMENTATION PAGE

Form Approved
OMB No. 0704-0188

1. REPORT DATE *(DD-MM-YYYY)*	2. REPORT TYPE	3. DATES COVERED *(From - To)*
01-10-2010	Supplemental Report	2004-2009

4. TITLE AND SUBTITLE

ESTCP WP-0411
"Optimized Deposition Parameters & Coating Properties of Cobalt Phosphorus Alloy Electroplating for Technology Insertion Risk Reduction"

5a. CONTRACT NUMBER

5b. GRANT NUMBER

5c. PROGRAM ELEMENT NUMBER

6. AUTHOR(S)

Ruben Prado, John Benfer, Diana Facchini, Keith Legg

5d. PROJECT NUMBER

5e. TASK NUMBER

5f. WORK UNIT NUMBER

7. PERFORMING ORGANIZATION NAME(S) AND ADDRESS(ES)

NAVAIR ISSC/FRC-SE
NAS Jacksonville
Bldg 793, Code 434
Jacksonville, FL 32212

8. PERFORMING ORGANIZATION REPORT NUMBER

WP-0411 Supplemental Report

9. SPONSORING / MONITORING AGENCY NAME(S) AND ADDRESS(ES)

Environmental Security Technology Certification Program Office
901 North Stuart Street, Suite 303
Arlington, VA 22203
Tel: (703) 696-2117

10. SPONSOR/MONITOR'S ACRONYM(S)

ESTCP

11. SPONSOR/MONITOR'S REPORT NUMBER(S)

WP-0411 Supplemental Report

12. DISTRIBUTION / AVAILABILITY STATEMENT

Approved for public release; distribution is unlimited.

13. SUPPLEMENTARY NOTES

14. ABSTRACT

Optimized plating deposition parameters were obtained using a Design of Experiment (DOE) approach. These parameters were validated through supplemental testing and found to be non-embrittling with improved fatigue and neutral salt fog corrosion performance as compared to hard chromium electroplate. The nCoP deposit did exhibit reduced hardness (560 VHN) and reduced taber wear abrasion performance as compared to hard chromium electroplate.
Producibility evaluations were performed utilizing a J52 Shaft section and a J52 Coupling component. Optimized plating parameters were successfully demonstrated on both ID & OD areas. The above plated components were then finished machined at FRC-SE with no observable defects.

15. SUBJECT TERMS

Electroplating, Chromium, Replacement, Cobalt, Phosphorus, Alloy, Nano-crystalline

16. SECURITY CLASSIFICATION OF:			17. LIMITATION OF ABSTRACT	18. NUMBER OF PAGES	19a. NAME OF RESPONSIBLE PERSON
a. REPORT	b. ABSTRACT	c. THIS PAGE			John E. Benfer
Unclassified	Unclassified	Unclassified	SAR	50	19b. TELEPHONE NUMBER *(include area code)* (904) 790-6405

Table of Contents

1.0 INTRODUCTION

1.1 BACKGROUND

At the conclusion of SERDP program (PP-1152) to develop Nanocrystalline Cobalt Phosphorus Alloy Plating (nCo-P) as an alternative to hard chrome plating for IDs, the coating exhibited good wear and corrosion resistance, with no hydrogen embrittlement (even without heat treating) and a fatigue debit similar to that of hard chromium electroplate (EHC).

At the beginning of the ESTCP program (WP-0411) the deposition conditions were adjusted to make the coating coverage more uniform between the edges and center of flat specimens (i.e. more uniform as a function of current density). After a considerable amount of development and testing both at Integran Technologies Inc. and at NAVAIR Jacksonville, the team had resolved most of these issues.

Subsequent hydrogen embrittlement testing of samples performed with new deposition conditions resulted in a coating that was embrittling to high strength steel substrates with or without embrittlement relief baking. Furthermore, the fatigue data set generated with the above deposition conditions was rejected due to invalid failure locations in the samples.

1.2 OBJECTIVES

The goals of this study were to define and optimize the process window for producing a high quality non-embrittling coating and to also perform a rapid fatigue analysis screening via rotating beam test protocol. In pursuit of these objectives, the following tasks were performed:

- *Process Window Definition* and plating parameter optimization using a design of experiments approach
- *Data Acquisition* using the optimized plating parameters
- *Producibility Evaluation* using the optimized plating parameters
- *Cost Benefit Analysis* using the optimized plating parameters

2.0 PROCESS WINDOW

2.1 METHODS

2.1.1 Design of Experiments

The process window was determined using a standard Design of Experiment (DOE) approach. Input variables were current density, pulse frequency and duty cycle. The plating bath was operated as specified by the Technical Data Sheet by Integran Technologies Inc. which includes optimized ranges for plating parameters and resulting material properties. Two experiments were conducted:

1. Exploratory DOE: The exploratory DOE was designed to define the initial operating window and the effects of operating variables on deposit properties. Here, a 2^3 full factorial design with a centerpoint was used, as shown in ***Table 1***. (high=1, low=-1, center pt=0)

2. Optimized DOE: Following the exploratory DOE, the optimized DOE was designed to downselect the final plating parameters for data acquisition, producibility and cost-benefit tasks. Here, a L8 mixed 2-4 level design was used, as shown in ***Table 2***.
   (For CD: low=1, mid-low=2, mid-high=3, high=4. For Frequency: low=0, high=1. For Duty Cycle: high=0, low=1)

TABLE 1
EXPLORATORY DOE INPUT VARIABLES.

Coded Variables		
Current Density	**Frequency**	**Duty Cycle**
1	1	1
1	1	-1
1	-1	1
1	-1	-1
-1	1	1
-1	1	-1
-1	-1	1
-1	-1	-1
0	0	0

TABLE 2
OPTIMIZED DOE INPUT VARIABLES.

Coded Variables		
Current Density	**Frequency**	**Duty Cycle**
1	0	0
2	0	0
3	0	0
4	0	0
1	1	1
2	1	1
3	1	1
4	1	1

The output variables are described in detail below. They included appearance, composition and microstructure, adhesion, current efficiency, thickness, hardness, internal stress, and hydrogen embrittlement. Experimental design and data analysis was performed with the aid of Minitab statistical software.

2.1.2 Sample Preparation

Three types of coupons were prepared using the plating conditions defined in ***Table 1*** & ***Table 2*** for use in subsequent tests. ***Figure 1*** illustrates coupon types as described below:

a) *Flat Coupons:* 1”x4” ASTM A36 (similar to AISI 1018/mild steel) coupons coated on one side with 0.010” in thickness nCo-P.

b) *Stress Strips:* thin copper strips with two legs that are epoxy coated on opposing sides. When opposing sides of legs are plated, the legs deflect under the stress of the coating.

c) *Hydrogen embrittlement bars:* ASTM F519, Type 1a1 bars, coated on a 1” section centered on the gage (i.e. 0.5” above/below gage) with 0.003” in thickness nCo-P. Four bars per plating condition. Hydrogen relief baking was not performed on the Exploratory DOE samples. For the Optimized DOE samples, a hydrogen relief bake at 375ºF for 24 hr was applied within 1 hr of plating.

(a) (b) (c)

FIGURE 1. IMAGES OF TEST COUPONS, INCLUDING (A) FLAT COUPONS, (B) STRESS STRIPS AND (C) HYDROGEN EMBRITTLEMENT BARS.

2.1.3 Appearance

Flat coupons were visually examined for coating uniformity, nodules, dendrites, pits, pores, cracks and other defects.

2.1.4 Composition and Microstructure

Composition and microstructure evaluations were conducted on the flat coupons. The composition of the deposits was determined using Energy Dispersion Spectroscopy (EDS). The crystal structure and grain size of the coatings was characterized using X-ray diffraction (XRD) techniques. A specific coating composition was not targeted. Rather, the composition was monitored to verify that there were no detrimental effects due to the changes in the operating conditions.

2.1.5 Adhesion

Adhesion testing was conducted on the flat coupons per ASTM B571 (“Standard Practice for Qualitative Adhesion Testing of Metallic Coatings”). Coupons were bent repeatedly, back and forth, through an angle of 180° until failure of the basis metal occurred. The fractured region was then examined at low magnification for separation or peeling of the coating. Attempts were then made to pry the coating with a sharp blade to assess whether there was any lift off of the coating which would indicate unsatisfactory adhesion.

2.1.6 Current Efficiency and Thickness

Plating efficiency and thickness were evaluated on the flat coupons. The plating efficiency was calculated for each of the samples by recording the mass of the sample before and after plating to obtain the total mass of the coating. The theoretical mass, m_t, was calculated using Faraday’s Law:

$$m_t = \frac{\frac{M_{Co}}{n} \cdot A \cdot i \cdot t}{F} \quad (1)$$

where:

M_{Co} is the atomic mass of cobalt
n is the valence of cobalt
A is the plating area
i is the current density
t is the plating time
F is Faraday's constant

The cathode current efficiency, CCE, was then calculated by:

$$CCE = \frac{m_a}{m_t} \quad (2)$$

where:

m_a is the measured coating mass

Coating thickness was determined by calculating the difference in thickness of the flat coupons before and after plating, as measured with a micrometer.

Throwing power was not explicitly evaluated as part of the DOE, however, it was assessed as part of the producibility evaluation using the down selected plating parameters.

2.1.7 Hardness

Hardness was evaluated on metallographically prepared cross-sections of the flat coupons. The microhardness of the coatings was determined using a Vickers Indenter with a 100 g load.

2.1.8 Internal Stress

Internal stress was evaluated on the stress strips. The deflection of the strips was measured using a deposit stress analyzer. This was then used to calculate the internal stress, S, according to:

$$S = \frac{UD}{3W} K \quad (3)$$

where:

U is the measured deflection of the strips
D is the coating density
W is the coating weight
K is the strip calibration constant

2.1.9 Hydrogen embrittlement

Hydrogen embrittlement testing was conducted in accordance with ASTM F519 ("Standard Test Method for Mechanical Hydrogen Embrittlement Evaluation of Plating/Coating Processes and Service Environments"). Hydrogen embrittlement bars were subjected to a sustained tensile load of 75% of the notch fracture strength (NFS) until (a) failure or (b) 200 hr had elapsed. For the Exploratory DOE only, samples sustaining 200 hr loading were then step-loaded in increments of 5% NFS per hour until failure. Results were therefore expressed in time to failure or % NFS.

The exploratory DOE for hydrogen embrittlement testing was utilized as a screening tool to identify near-optimized plating ranges. Step-load increases were performed on coupon sets that passed the hydrogen embrittlement criteria to increase the fidelity of the obtained data. The hydrogen embrittlement testing conducted as a part of the follow-on optimization DOE was intended to confirm that the selected optimized plating conditions satisfied HE pass/fail criteria.

2.2 RESULTS – EXPLORATORY DOE

2.2.1 Appearance

Results of the appearance evaluations are summarized in ***Table 3***. Uniformly smooth and shiny deposits were produced at all plating conditions tested. However, the severity of edge dendrites varied with plating conditions. ***Table 3*** ranks the samples in order of the severity of edge dendrites observed. The current density was found to have the most significant effects on edge dendrites, followed by duty cycle, then frequency. The most severe edge dendrites were produced with high current density, low duty cycle and low frequency.

TABLE 3
RESULTS OF APPEARANCE EVALUATIONS.

Factors			Responses	
Current Density	**Frequency**	**Duty Cycle**	**Rank[1]**	**Images**
1	-1	-1	1	
1	1	-1	2	
1	-1	1	3	
1	1	1	4	
0	0	0	5	

TABLE 3 (continued)
RESULTS OF APPEARANCE EVALUATIONS

Factors			Responses	
Current Density	**Frequency**	**Duty Cycle**	**Rank[1]**	**Images**
-1	-1	-1	6	
-1	1	-1	7	
-1	-1	1	8	
-1	1	1	9	

[1] Rank: most severe edge dendrites to least severe edge dendrites.

2.2.2 Composition and Microstructure

The results of the composition and microstructure testing are summarized in ***Table 4***. Statistical evaluations of the data indicate that the deposit phosphorus content increases with decreasing current density, but does not vary with frequency or duty cycle in the ranges evaluated.

All deposits were found to be nanocrystalline, with a hexagonally close packed grain structure. Neither the grain size nor the microstructure was found to vary with current density, frequency or duty cycle in the ranges evaluated.

TABLE 4
RESULTS OF COMPOSITION AND MICROSTRUCTURE EVALUATIONS.

Factors			***Responses***		
Current Density	**Frequency**	**Duty Cycle**	**Composition (wt%P)**	**Grain size (nm)**	**Microstructure**
1	1	1	1.2±0.1	6	Nanocrystalline
1	1	-1	1.1±0.2	5	Nanocrystalline
1	-1	1	1.1±0.1	5	Nanocrystalline
1	-1	-1	1.1±0.1	5	Nanocrystalline
-1	1	1	1.4±0.1	8	Nanocrystalline
-1	1	-1	1.5±0.1	8	Nanocrystalline
-1	-1	1	1.3±0.1	8	Nanocrystalline
-1	-1	-1	1.4±0.1	8	Nanocrystalline
0	0	0	1.2±0.1	6	Nanocrystalline

2.2.3 Adhesion

The results of the adhesion testing are summarized in ***Table 5***. Two failures were observed, however these did not correlate with any of the operating conditions. Therefore, it is suspected that activation process rather than the plating process was responsible for the adhesion failures. The activation process is an immersion for 3 minutes in an acid dip. It is susceptible to contamination.

TABLE 5
RESULTS OF ADHESION EVALUATION.

Factors			Responses
Current Density	**Frequency**	**Duty Cycle**	**Adhesion (Pass/Fail)**
1	1	1	Pass
1	1	-1	Pass
1	-1	1	Pass
1	-1	-1	Fail
-1	1	1	Pass
-1	1	-1	Pass
-1	-1	1	Fail
-1	-1	-1	Pass
0	0	0	Pass

2.2.4 Current Efficiency and Thickness

The results of the current efficiency and thickness testing are summarized in ***Table 6***. Statistical evaluations of the data indicate that current efficiency does not vary with current density, frequency or duty cycle in the ranges evaluated. Thickness was found to decrease with decreasing current density (for the same plating time) but did not vary with frequency or duty cycle in the ranges evaluated. The thickness distribution was found to vary with duty cycle, with lower duty cycles resulting in increased edge buildup.

TABLE 6
RESULTS OF CURRENT EFFICIENCY AND THICKNESS EVALUATIONS.

Factors			Responses	
Current Density	**Frequency**	**Duty Cycle**	**Thickness (thou)**	**Current Efficiency (%)**
1	1	1	11.4	80
1	1	-1	7.2	73
1	-1	1	12.4	90
1	-1	-1	7.2	85
-1	1	1	8.0	81
-1	1	-1	8.6	83
-1	-1	1	9.1	86
-1	-1	-1	7.4	77
0	0	0	12.2	84

2.2.5 Hardness

The results of the hardness testing are summarized in ***Table 7***. Statistical evaluations of the data indicate that hardness increases with decreasing current density, but does not vary with frequency or duty cycle in the ranges evaluated.

TABLE 7
RESULTS OF HARDNESS EVALUATION.

Factors			*Responses*
Current Density	**Frequency**	**Duty Cycle**	**Hardness (VHN)**
1	1	1	506
1	1	-1	499
1	-1	1	515
1	-1	-1	528
-1	1	1	534
-1	1	-1	537
-1	-1	1	536
-1	-1	-1	546
0	0	0	515

2.2.6 Internal Stress

The results of the internal stress testing are summarized in ***Table 8.*** A tensile residual stress was observed for all plating conditions evaluated. Statistical evaluations of the data indicate that residual stress does not vary with current density, frequency or duty cycle in the ranges evaluated.

TABLE 8
RESULTS OF RESIDUAL STRESS EVALUATION.

Factors			*Responses*
Current Density	**Frequency**	**Duty Cycle**	**Residual stress (ksi)**
1	1	1	13.6
1	1	-1	13.5
1	-1	1	13.3
1	-1	-1	12.0
-1	1	1	14.6
-1	1	-1	12.2
-1	-1	1	15.2
-1	-1	-1	13.8
0	0	0	14.2

2.2.7 Hydrogen embrittlement

The results of the hydrogen embrittlement testing are summarized in ***Table 9***. Results are shown as time to failure (hours) for bars that failed prior to the 200 hr threshold, or as %NFS at failure for bars that surpassed the 200 hr threshold and were subsequently step-loaded.

Despite having not been baked for hydrogen embrittlement relief after the coating was applied, over 50% of the samples tested were able to sustain the 75% NFS load for 200 hr. Statistical evaluations of the data indicate that hydrogen embrittlement does not vary with current density, frequency or duty cycle in the ranges evaluated.

TABLE 9
RESULTS OF HYDROGEN EMBRITTLEMENT EVALUATION.

Factors			Responses			
Current Density	Frequency	Duty Cycle	Hydrogen Embrittlement (hours to failure or % NFS)			
			Bar 1	Bar 2	Bar 3	Bar 4
1	1	1	40	121	193	193.1
1	1	-1	85%	100%	100%	100%
1	-1	1	49	57	58	80%
1	-1	-1	85%	90%	90%	100%
-1	1	1	136	193	200	80%
-1	1	-1	80	80	121	193
-1	-1	1	85%	100%	100%	100%
-1	-1	-1	85%	90%	100%	100%
0	0	0	80	123	137	80%

2.2.8 Summary and Conclusions

Several properties were found to be independent of the plating parameters, including: current efficiency, hydrogen embrittlement, internal stress, adhesion and microstructure. Composition and hardness were found to vary with current density. Severity of edge dendrites were found to vary with all parameters evaluated.

For further evaluation in the optimization DOE, four current densities were selected with two pulsing conditions as input variables. The output variables remained unchanged.

2.3 RESULTS – OPTIMIZATION DOE

2.3.1 Appearance

Results of the appearance evaluation are shown in ***Table 10***. Deposits were found to be generally uniformly smooth and shiny, however surface nodules formed at low current density for both pulse conditions. These were found to be less severe at the lower duty cycle. As was previously observed, the severity of the edge dendrites increased with increasing current density. The edge dendrites were the most severe for the low duty

cycle/high frequency condition. These results are consistent with those previously obtained for the Exploratory DOE.

TABLE 10
RESULTS OF THE APPEARANCE EVALUATION.

Current Density	Pulse Condition 0	Pulse Condition 1
1		
2		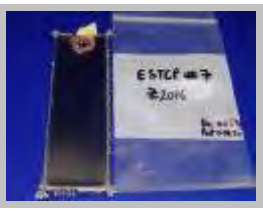
3		
4		

2.3.2 Composition and Microstructure

The results of the composition and microstructure testing are summarized in ***Table 11***. Statistical analysis of the results indicate that the deposit phosphorus content increases with decreasing current density, but does not vary with pulse conditions.

All samples were found to be nanocrystalline, with a hexagonally close-packed microstructure. Statistical analysis of the results indicates that the grain size and microstructure do not vary with current density or pulse conditions. Results obtained here for the composition and microstructure are consistent with the trends observed for the Exploratory DOE.

TABLE 11
RESULTS OF THE COMPOSITION AND MICROSTRUCTURE EVALUATIONS.

Factors			*Responses*		
Current Density	**Frequency**	**Duty Cycle**	**Composition (wt%P)**	**Grain size (nm)**	**Microstructure**
1	0	0	1.9±0.1	15	Nanocrystalline
2	0	0	1.9±0.1	11	Nanocrystalline
3	0	0	1.9±0.2	8	Nanocrystalline
4	0	0	1.6±0.1	8	Nanocrystalline
1	1	1	2.1±0.1	12	Nanocrystalline
2	1	1	1.9±0.1	11	Nanocrystalline
3	1	1	1.9±0.2	10	Nanocrystalline
4	1	1	1.8±0.1	8	Nanocrystalline

2.3.3 Adhesion

The results of the adhesion testing are summarized in ***Table 12***. Two failures were observed, however these did not correlate with any of the operating conditions. Therefore, it is suspected that the activation process (i.e. inadequate surface preparation due to operator error) rather than the plating process was responsible for the adhesion failures.

TABLE 12
RESULTS OF THE ADHESION EVALUATION.

Factors			*Responses*
Current Density	**Frequency**	**Duty Cycle**	**Adhesion (pass/fail)**
1	0	0	Fail
2	0	0	Pass
3	0	0	Pass
4	0	0	Fail
1	1	1	Pass
2	1	1	Pass
3	1	1	Pass
4	1	1	Pass

2.3.4 Current Efficiency and Thickness

The results of the current efficiency and thickness testing are summarized in ***Table 13***. Statistical evaluations of the data indicate that current efficiency does not vary with current density, frequency or duty cycle in the ranges evaluated. Thickness was found to decrease with decreasing current density (for the same plating time) but did not vary with frequency or duty cycle in the ranges evaluated. These results are consistent with the trends observed for the Exploratory DOE.

TABLE 13
RESULTS OF THE CURRENT EFFICIENCY AND THICKNESS EVALUATIONS.

Factors			*Responses*	
Current Density	**Frequency**	**Duty Cycle**	**Thickness (thou)**	**Current Efficiency (%)**
1	0	0	10.6	90
2	0	0	9.2	89
3	0	0	9.7	90
4	0	0	10.2	87
1	1	1	12.1	89
2	1	1	9.0	89
3	1	1	10.9	86
4	1	1	10.0	90

2.3.5 Hardness

The results of the hardness testing are summarized in ***Table 14***. Statistical analysis of the results indicates that the hardness increases with decreasing current density, but does not vary with pulse conditions. These results are consistent with the trends observed for the Exploratory DOE.

TABLE 14
RESULTS OF THE HARDNESS EVALUATION.

Factors			*Responses*
Current Density	**Frequency**	**Duty Cycle**	**Hardness (VHN)**
1	0	0	591
2	0	0	574
3	0	0	560
4	0	0	547
1	1	1	586
2	1	1	567
3	1	1	557
4	1	1	549

2.3.6 Hydrogen Embrittlement

Property evaluations revealed that only the edge dendrite severity varied with the pulsing conditions, and that the low duty cycle condition was preferred to minimize their severity. Mid-range current densities were preferred to increase the hardness and maintain a uniformly smooth and shiny appearance.

As a final screening, hydrogen embrittlement testing was conducted on samples produced using the low duty cycle condition at current densities of mid-low, mid-high and high. Within 1 hr of plating, test samples were baked at 375ºF for 24 hr. Hydrogen embrittlement testing was then conducted per the methods described in Section 2.1.9. All samples were found to sustain the 75% NFS load for 200 hr, indicating that the coatings passed hydrogen embrittlement testing.

2.3.7 Summary and Conclusions

The final downselected plating parameters were a duty cycle and frequency of low and a current density of mid-high.

3.0 DATA ACQUISITION

Once the process window had been established, additional data were obtained with the new optimized deposition conditions.

3.1 METHODS

3.1.1 Microstructure and stress

Microstructure and stress were evaluated per the methods described in Section 2.1.4 and Section 2.1.8, respectively.

3.1.2 Adhesion

Adhesion was evaluated per the methods described in Section 2.1.5.

3.1.3 Porosity Test

Flat coupons were cross-sectioned and examined using optical and scanning electron microscopes for signs of voids and porosity.

3.1.4 Hydrogen Embrittlement

Hydrogen embrittlement testing was conducted per the methods described in Section 2.1.9. Within 1 hr of plating, test samples were baked at 375ºF for 24 hr. In an industrial setting, baking could occur up to 4 hrs prior to plating, provided the part is not subjected to stresses.

3.1.5 Corrosion

Corrosion testing was conducted in accordance with ASTM B117 (“Standard Practice for Operating Salt Spray (Fog) Apparatus”). Two mild steel coupons (4”x4”) were coated on one side with 0.003” nCo-P at Integran Technologies Inc. and two mild steel coupons (4”x4”) were coated with 0.003” EHC at FRC-SE. The backs and sides of the coupons were masked to prevent uncoated steel from being exposed to the test. Samples were left in the as deposit condition and subjected to salt spray testing for 165 hrs. Following testing, samples were visually examined for signs of red rust. The surface composition of the samples was also evaluated by µ-EDXRF for the presence of iron.

3.1.6 Fatigue

Fatigue testing consisted of rotating beam fatigue in lieu of axial fatigue testing as defined the whitepaper proposal to minimize cost and to improve the turnaround time of the fatigue data. Fatigue testing was conducted on bare, nCo-P-coated and EHC-coated test samples. Test samples were 4340 steel (260-280 ksi) hourglass bars as shown in ***Figure 2***, and their surfaces were unpeened. The unpeened condition was

motivated in order to meet NAVAIR approval requirements and to better understand the fatigue sensitivity of the coating without introducing additional external variables. Twenty specimens were coated with 0.006" nCo-P at Integran Technologies Inc., twenty were coated with 0.006" EHC at FRC-SE, and twenty remained bare. Coatings were ground to 0.003" using low-stress grinding techniques, and were longitudinally polished to a 16 µinch Ra finish.

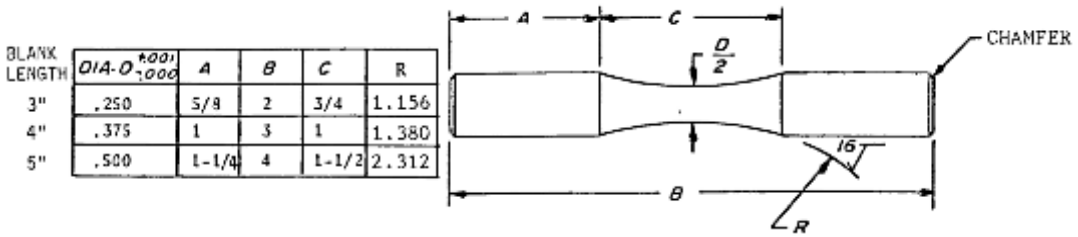

FIGURE 2. ROTATING BEAM FATIGUE BAR GEOMETRY.

Rotating beam fatigue testing was conducted in laboratory air at ambient temperature. Loads were spread between 85% of tensile yield strength (Fty) and the runout load (10^7 cycles), with no more than four points per load. Load and cycles to failure were used to generate S-N curves for bare, nCo-P-coated and EHC-coated specimens.

3.1.7 Immersion testing

Fluid compatibility was not expected to change significantly, as the deposit microstructure and composition has not changed significantly. The optional fluid immersion testing was therefore not conducted in this study. It was expected to be revisited during the next stage of the program.

3.1.8 Wear and hardness testing

Hardness was evaluated per the methods described in Section 2.1.7.

Abrasive wear resistances of the nCo-P and EHC baseline were evaluated by Taber wear testing in accordance with ASTM D4060 ("Standard Test Method for Abrasion Resistance of Organic Coatings by the Taber Abraser"). Flat mild steel coupons (4"x4") were coated with 0.002" nCo-P at Integran Technologies Inc. or 0.002" at FRC-SE. Testing was conducted using CS-17 wheels at FRC-SE.

3.2 RESULTS

3.2.1 Microstructure and stress

Figure 3 shows a portion of the X-ray diffraction pattern for the nCo-P deposit. The deposit was found to be nanocrystalline, with the HCP crystal structure typically found in cobalt, and an average grain size of 8 nm.

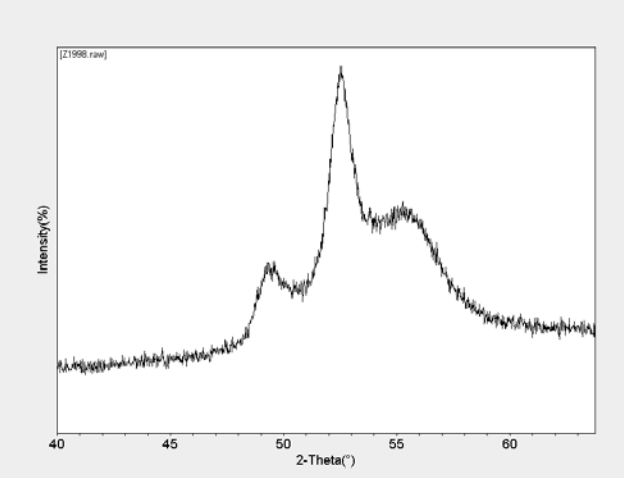

FIGURE 3. PORTION OF THE X-RAY DIFFRACTION PATTERN FOR NCO-P DEPOSIT PRODUCED WITH THE OPTIMIZED PLATING CONDITIONS.

Deposit stress was found to be 10-15ksi tensile.

3.2.2 Adhesion

As shown in ***Figure 4.***, examination of the fractured surface revealed no signs of coating delamination or flaking, indicating that the sample passes adhesion testing.

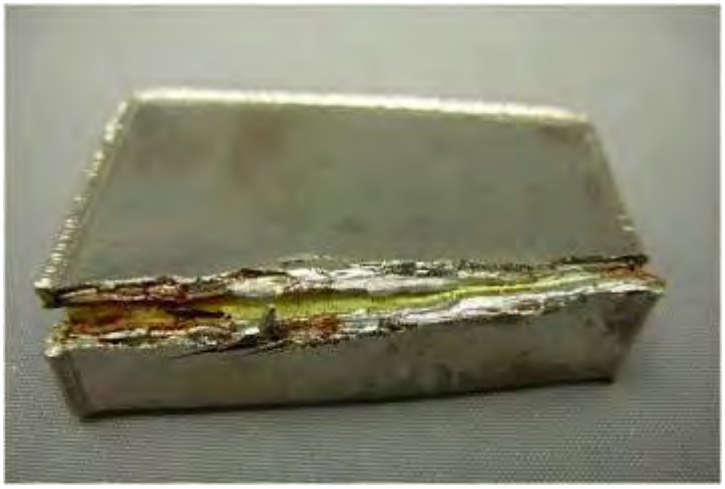

FIGURE 4. IMAGE OF THE FRACTURE SURFACE FOLLOWING BENDING.

3.2.3 Porosity Test

As shown in ***Figure 5*** examination of the coating cross-section revealed no signs of cracks pores or voids, indicating that the sample is free of gross porosity. This is in contrast to EHC, which exhibits microcracking.

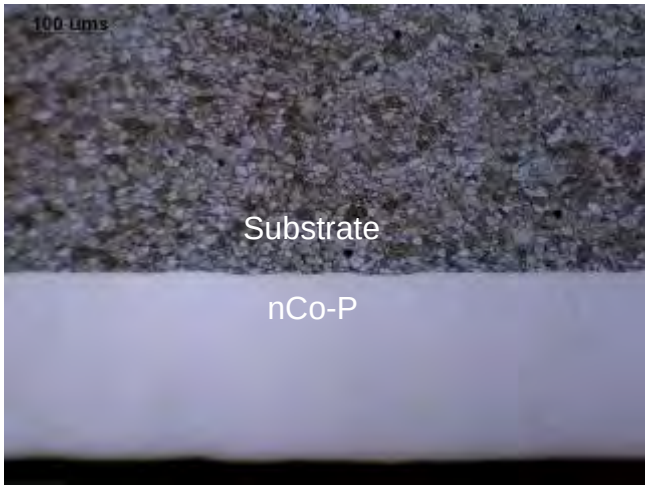

FIGURE 5. OPTICAL MICROGRAPH OF THE CROSS-SECTION OF THE NCO-P DEPOSIT USING NITAL ETCHANT.

3.2.4 Hydrogen Embrittlement

No failures were noted after 200 h at the sustained load of 75% NFS, indicating that the coating passes hydrogen embrittlement. This behavior is similar to that of EHC, which is known to pass hydrogen embrittlement testing when a similar bakeout is performed following plating.

3.2.5 Corrosion

As shown in ***Figure 6a***, examination of the EHC-coated panels following 165 h salt fog exposure reveals an orange/brown discoloration across the entire panel. Surface composition analysis reveals the presence of iron and chromium, as shown by the µ-EDXRF spectra in ***Figure 6a*** indicating that red rust has formed. By contrast, the nCoP-coated panels following salt fog exposure exhibit a golden brown discoloration. Surface composition analysis reveals the presence of cobalt, but with no iron as shown by the µ-EDXRF spectra in ***Figure 6b*** indicating the absence of red rust but likely a surface oxide. These results indicate that nCo-P exhibits superior corrosion resistance to EHC.

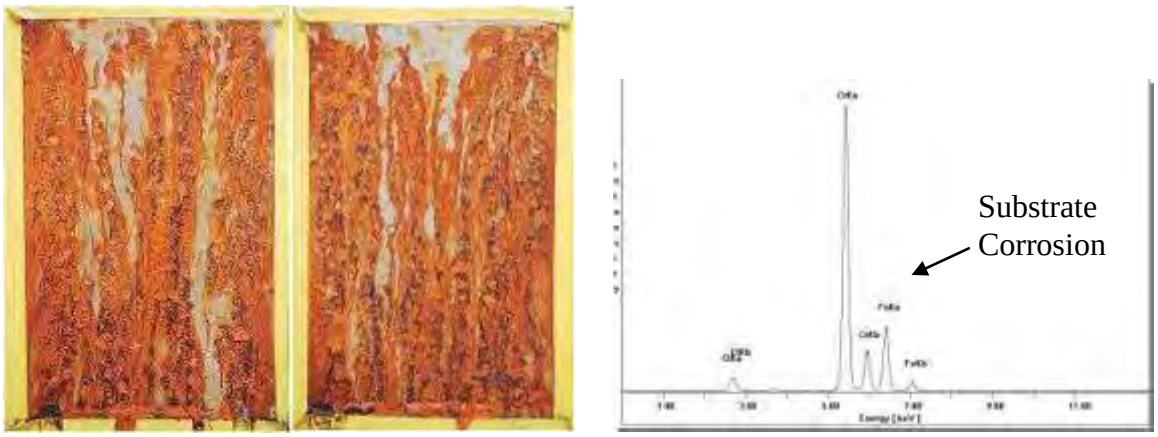

(a)

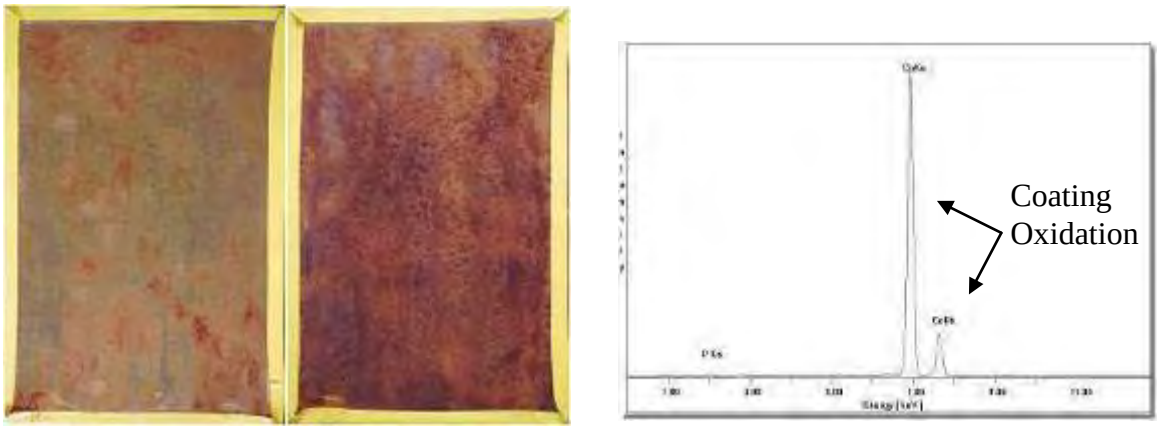

(b)

FIGURE 6. IMAGES AND μ-EDXRF SPECTRA FOR THE SURFACES OF (A) EHC- COATED AND (B) NCO-P-COATED MILD STEEL FOLLOWING 165H SALT FOG EXPOSURE.

3.2.6 Fatigue

As shown in ***Figure 7*** below, fatigue data shows a significant fatigue debit for EHC coating compared to bare material. In comparison, the nCo-P coating shows a fatigue life similar to the bare material at lower loads. At lower applied loads there appears to be a debit compared to bare, however, this is not nearly as severe as the debit exhibited by the EHC coated material. Therefore, nCo-P exhibits significantly enhanced fatigue performance compared to EHC.

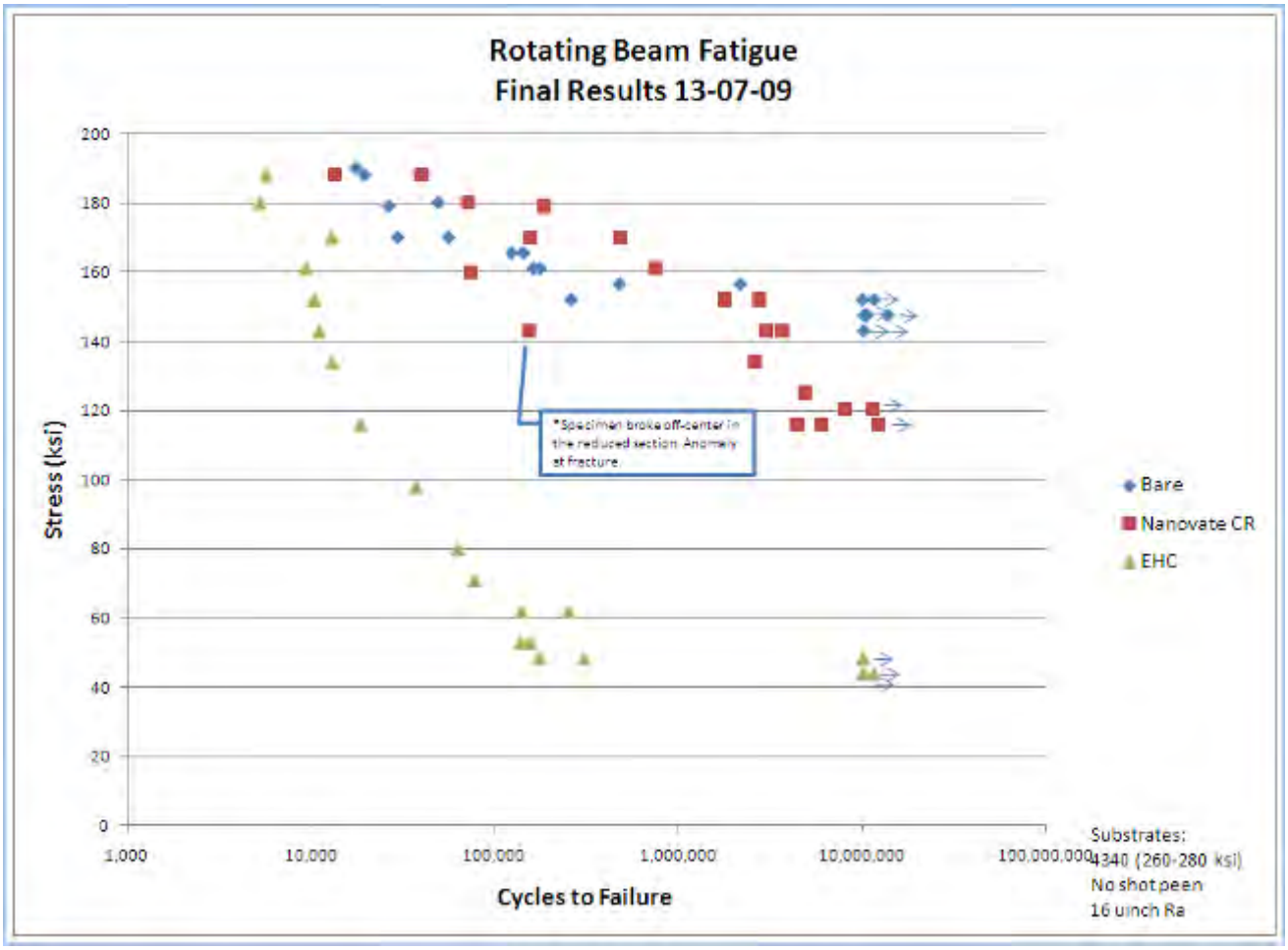

FIGURE 7. ROTATING BEAM FATIGUE RESULTS SHOWN AS AN S-N CURVE.

3.2.7 Wear and hardness testing

The microhardness was found to be 560 VHN as-deposited. The results indicate that nCo-P has lower hardness than EHC.

The results of the Taber Wear test are shown in ***Table 15***. The Taber Wear Index was found to be 17.23 mg/1000 cycles for nCoP, and 4.15 mg/1000 cycles for EHC, indicating that EHC has superior abrasive wear performance to nCo-P.

TABLE 15
TABER WEAR TEST RESULTS FOR NCO-P & EHC COUPONS.

Cycles	Weight (g)			
	nCo-P Coupon #3RZ2057	nCo-P Coupon #4LZ2056	Cr Coupon #3L	Cr Coupon #4R
0	128.7596	131.1900	118.1269	121.4091
1000	128.7399	131.1713	118.1206	121.4052
2000	128.7218	131.1539	118.1167	121.3975
3000	128.7047	131.1367	118.1143	121.3938
4000	128.6855	131.1219	118.1068	121.3906
5000	128.6684	131.1034	118.1051	121.3869
6000	128.6525	131.0859	118.1015	121.3819
7000	128.6346	131.0704	118.0977	121.3777
8000	128.6175	131.0545	118.0951	121.3727
9000	128.6016	131.0378	118.0873	121.3726
10000	128.5850	131.0200	118.0865	121.3666
Total Wt Loss (mg/1000 cycles)	**17.46**	**17.0**	**4.04**	**4.25**

3.3 SUMMARY AND DISCUSSION

Type of Performance Objective	Primary Performance Criteria	Expected Performance (Metric)	Result	Actual Performance Objective Met?
Quantitative	Internal Stress	No specific requirement.	10-15 ksi	-
Quantitative	Microstructure	Microstructure includes items such as grain size and crystal structure. For nCo-P coatings, grain size shall be less than 100 nm and crystal structure shall be HCP.	Nanocrystalline (8 nm grain size), hexagonal close-packed structure	Yes
Quantitative	Microhardness	Microhardness of as-deposited coatings shall be no less than 650 VHN. Microhardness shall be capable of being controlled through heat treatment up to 800 VHN.	560 VHN (as-deposited)	No
Qualitative	Porosity	Coatings shall be free of pits, pores and microcracks when observed microscopically.	No cracks, pores or voids	Yes
Quantitative	Fatigue	Low-cycle and high-cycle rotating beam fatigue testing shall be conducted for nCo-P coatings of 0.003" thickness on 4340 steel substrates heat treated to 260-280 ksi. Cycles-to-failure at different stress levels shall be determined and standard S/N curves shall be generated. The S/N curves for the nCo-P coatings shall lie on or above those for EHC coatings.	Credit vs. EHC. Comparable to bare at LCF, debit compared to bare at HCF.	Yes
Quantitative	Wear	Abrasive wear tests shall be conducted using the Taber wear test apparatus in accordance with ASTM D4060 using a CS-17 wheel. The wear rate of the nCo-P coating shall be less than or equal to EHC.	17.23 mg/1000 cycles	No
Quantitative	Corrosion	In salt-fog corrosion tests, time until observing corrosion product for nCo-P coatings should be less or equal to time for EHC coatings (ASTM B117).	No red rust after 165 h	Yes
Quantitative	Hydrogen embrittlement	A coating thickness of 0.003" of nCo-P shall be deposited onto ultra-high-strength steel Type 1a1 ASTM F519 specimens. Specimens loaded to 75% of notch tensile stress must pass 200 hour test (after a hydrogen bake)	Passed 200 h sustained load	Yes
Qualitative	Adhesion	No spalling or delamination of the coating from the substrate when tested in accordance with ASTM B571.	No delamination or flaking	Yes

4.0 PRODUCIBILITY

Producibility testing was conducted by Integran Technologies Inc. using the optimized plating conditions due to hardware failures at FRC-SE. Components were provided by FRC-SE. The coating was applied to both internal diameter sections and outer diameter sections as described below.

4.1 INNER DIAMETER PLATING DEMONSTRATION

4.1.1 Component Description

The demonstration piece for internal diameter plating was a J52 coupling, as shown in ***Figure 8***. This part was 4340 steel and required plating on a small 1" wide band on the inner diameter of the part.

FIGURE 8. J52 COUPLING USED FOR THE INNER DIAMETER PLATING DEMONSTRATION.

4.1.2 Methods/Setup

A process flow chart shown in ***Figure 9*** summarizes the operations completed in preparing the demonstration part for plating. The demonstration part as-received did not require stripping of previous coatings on the desired plating area.

In order to mask the part for plating, several methods of masking were employed. First, the plating area was covered using generic black tape. Next, holes found on the bottom of the part were plugged with plastic plugs. Plugs were trimmed in order to facilitate application of maskants. Electroplating tape was used to mask the remaining holes on the surface. Enthone Stop-Off #1 was then applied by brushing and dipping and allowed to cure. Once the part was sufficiently masked, the plating area was uncovered by removing the black tape.

The area to be plated was then alconox scrubbed using a Scotch Brite pad. Use of higher mesh pads is recommended in order to reduce appearance of scratches in the final deposit. Next the part was attached to the plating rack. After checking for electrical continuity, the part was then immersed in the alkaline cleaning solution. It was then electrocleaned for 3 minutes at a current density of 50 mA/cm^2 followed by a rinsing step. The part was then activated using a mineral acid (5% HF/30% Sulfuric Acid) for 1 minute at an anodic current density of 300 mA/cm^2 (live entry). Following activation, the part was rinsed, and then plated with nCoP with the optimized pulse condition identified in Section 2.0. A flow eductor was attached in order to facilitate flow at the plating area. Following plating, the part was removed and rinsed. The part was then de-racked, and manually de-masked.

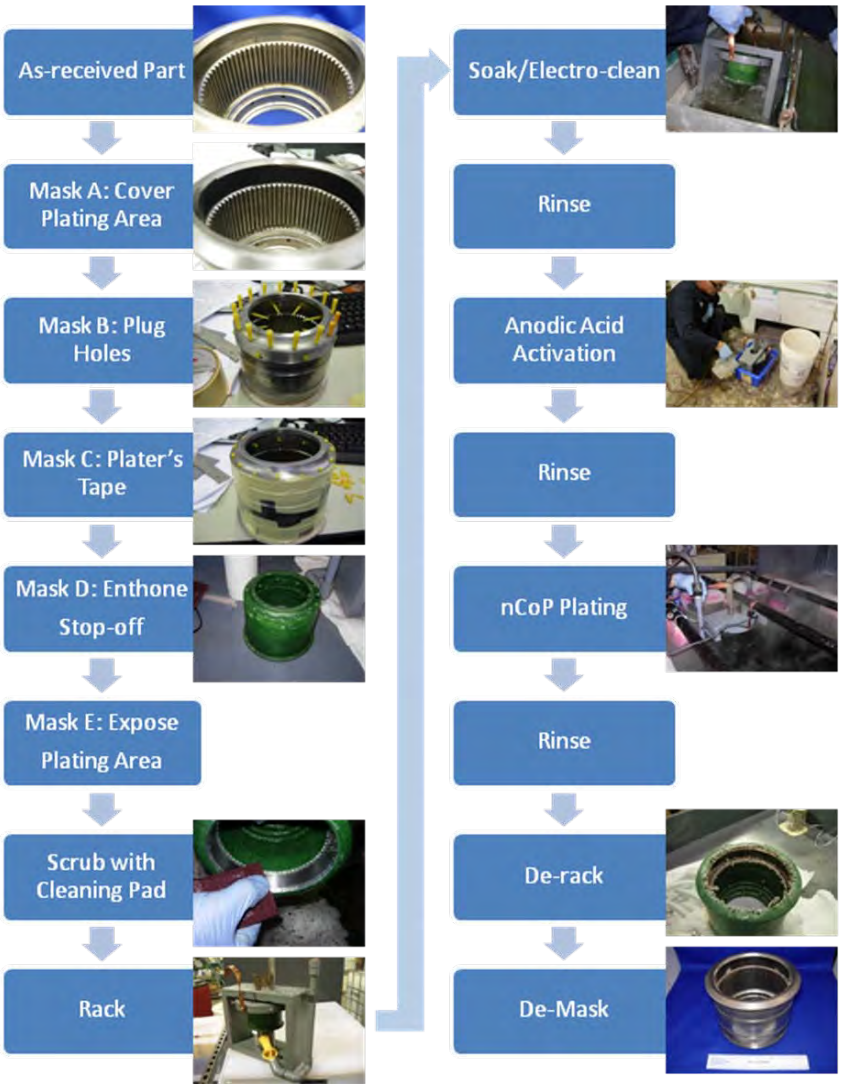

FIGURE 9. PROCESS FLOW CHART FOR J52 SHAFT ID PLATING.

4.1.3 Results

The as-deposited electroplate on the J52 coupling was smooth and shiny. No pits or cracks were observed. A few isolated nodules including some small dendrites were present along the plated edge of the ID which is not uncommon in areas where higher current densities are expected. Some imperfections were noted, consistent with how the part was received. The average as-deposit thickness was 0.011”± 0.00076”. Following plating, the part was machine ground to a surface finish of 16 microinches Ra or better. The aim of grinding the plated part was to evaluate machinability characteristics. A runout of the edges was not performed as this was not required for the evaluation.

J52 COUPLING FOLLOWING FRC-SE MACHINING OF ID PLATED AREA

4.2 OUTER DIAMETER PLATING DEMONSTRATION

4.2.1 Component Description

The demonstration piece for outer diameter plating was a J52 shaft (section), as shown in ***Figure 10***. This part was 4340 steel and required plating on a small 2" wide band on the outer diameter of the part.

FIGURE 10. J52 SHAFT (SECTION) USED FOR THE OUTER DIAMETER PLATING DEMONSTRATION.

4.2.2 Methods/Setup

A process flow chart shown in ***Figure 11*** summarizes the operations completed in preparing the demonstration part for plating. The demonstration part as received had a corroded surface where it was previously plated. In order to prepare the part for plating, the substrate was abrasively blasted using aluminum oxide media with a mesh size of 120. Upon inspecting the part, there was a pit present along the outline of the plated/non-plated interface.

In order to mask the part for plating, several methods of masking were employed. First, lead tape was adhered along the border of the area to be plated. Next, generic masking tape was applied to the area to be plated. This helped to prevent any maskant from covering the plating surface. The rack, consisting of two threaded rods and two hose clamps, was then connected to the part to allow for electrical contact. Then, using Electroplater's tape, the remaining uncovered areas were masked. Enthone Mask-off No.1 was then applied on top of the tape. The area to be plated was then uncovered by removing generic masking tape.

The area to be plated was scrubbed with a cleaning pad. Use of higher mesh pads is recommended in order to reduce appearance of scratches in the final deposit. Next the

part was immersed in the alkaline cleaning solution. It was electrocleaned for 3 minutes at a current density of 50 mA/cm^2. The part was rinsed and then attached to a rotator assembly. The part was activated using a mineral acid (5% HF/30% Sulfuric Acid) for 1 minute at an anodic current density of 300 mA/cm^2 (live entry). The part was rinsed and then plated with nCo-P with the optimized pulse condition Section 2.0. A flow eductor is attached in order to facilitate flow at the plating area. Once plating was complete, the rotation was stopped, the part was removed and was rinsed. Finally, the part was de-racked and manually de-masked.

FIGURE 11. PROCESS FLOW CHART FOR J52 SHAFT OD PLATING.

4.2.3 Results

Many small nodules were scattered along the surface of the plated J52 Shaft. This is consistent with electroplating of thick coatings. Some small dendrites were seen along the plated edges which is typical in high current density areas. Some imperfections were noted, consistent with how the part was received. The average deposit thickness prior to machining was 0.014”± 0.0001”. Following plating, the part was machine ground to a surface finish of 16 microinches Ra or better. The aim of grinding the plated part was to evaluate machniability characteristics. A runout of the edges was not performed as this was not required for the evaluation.

J52 SHAFT SECTION FOLLOWING FRC-SE MACHINING OF OD PLATED AREA

5.0 COST BENEFIT ANALYSIS

5.1 BACKGROUND

This section contains a Cost Benefit Analysis carried out using the C-MAT (Calculation for Material Alternative Technologies) Decision Tool, whose development was funded by SERDP/ESTCP. Cost data has been reviewed to reflect new processing conditions (including current density, hence plating speed).

5.2 ASSUMPTIONS

1. The plating workload is based on the actual number of parts processed, taken from shop records, and an estimate of the average part size. Most calculations in the present analysis (except environmental costs) therefore reflect the cost per square foot plated.
2. The workload is based on JAX chrome plating data for 2006 (see Table 16 - 18). Note that current OD plating approved for HVOF is being migrated. The nCoP coating is being considered for both ID & OD workload. Only the ID workload (all of which is J52 engine parts) for JAX chrome plating operations will be included as a worst-case scenario.
3. The calculations assume plating tank sizes of 1000 gals for each of the stripping, activation, and plating operations in both the Cr and nCo-P process lines. The masking tanks (wax for Cr, peel coat for nCo-P) are assumed to be smaller at 700 gals, and the Co anode tank for nCo-P only 10 gals.
4. It is assumed that the plating tanks are dummy plated once a month for Cr and once a week for nCo-P, and that each dummying requires 1 hr of labor.
5. 24/7 operation is assumed for:
    - Plating tank heating (by steam) for both Cr and nCo-P plating
    - Total water usage (makeup + rinse water)
    - The Cr^{6+} scrubber, and also EPA NESHAP monitoring of Cr^{6+} (monitoring actually required only when Cr plating operations occur)
6. Power required for the activation step is ignored in both cases, because it is small.
7. For nCo-P plating, it is assumed that the anodes will be Ti rods, Co plated in a special Co anode tank (rather than electrolytic Co squares in a basket). The rods will be plated to a thickness of 20 mils, enabling 10 ID parts to be plated from each anode rod in 1-2 runs.
8. Hazardous waste:

- At JAX, Cr^{6+} waste from all Cr stripping and chromating operations is combined with waste from the Cr plating line. But the Cr^{6+} waste numbers used in this analysis, including the $53,625 annual cost of scrubber energy and maintenance, are estimates for plating operations only.
- The quantity of Cr^{6+} solid waste is based on 2006 data. (This number has been decreasing annually as more Cr plating work is migrated to HVOF.)

9. EPA NESHAP non-compliance fines are not included in the environmental costs for Cr plating, since such fines have never been levied on JAX. However, the penalties are substantial resulting in $32,500 per day per violation.
10. OSHA monitoring costs for Cr plating are not included in the cost model either. This is because it has been found that the exposure level of plating personnel to Cr^{6+} under typical plating conditions barely registers on the monitoring equipment, so that ongoing monitoring is not required. However, an annual skin test is carried out.

TABLE 16
FRC-SE GENERAL COST DATA.

Cost item	Quantity	Unit	Source/Comments
Workload			
# ID parts Cr plated per year	85		NAVAIR FRCSE Production, 4/18/07
Average ID part plated area	0.4	sq ft	NAVAIR FRCSE Production, 4/18/07
ID plating workload	34	sq ft	Same workload assumed for nCo-P plating
OD plating workload	144	sq ft	NAVAIR FRCSE Production, 4/18/07
Total (ID + OD) workload	178	sq ft	
ID area ratio	19%		
OD area ratio	81%		OD workload gradually being migrated to HVOF
Average ID plating process time	8.43	hr	ISSC JAX Materials Engineering, 3/28/07 – includes 0.30 hr for baking step (both Cr and nCo-P) Actual process time depends on part configuration
Rates			
Labor rate - direct	$65.00	$/hr	NADEP JAX, 2005* – generic burdened rate
Material - indirect			1.74% of direct
Water utility rate	$0.00	$/gal	NADEP JAX, 2005* – rate used for rinse and makeup water
Electricity utility rate	$0.07	$/kWh	ISSC JAX Environmental Logistics, 3/6/07 – rate used for plating power
Steam utility rate	$ 1–1.50	$/hr	ISSC JAX Environmental Logistics, 3/28/07 – rate used for plating tank heater power (Cr – nCoP)
Inflation rate	0%		
Discount rate	3%		
Depreciable life of equipment	15	yr	
Salvage value	10%		
Hazardous waste disposal			
Cr^{6+} solid waste	$1.03	$/lb	NADEP JAX, 2005* – hazardous waste rate
Cr^{6+} rinsewater	$0.85	$/gal	NADEP JAX, 2005* – 2% of EHC rinsewater treated
nCo-P solid waste	$0.03	$/lb	NADEP JAX, 2005* – solid waste rate
nCo-P rinsewater	$0.85	$/gal	NADEP JAX, 2005* – 0.2% of nCo-P rinsewater assumed treated

** Data from "Infrared Reflectance Imaging Technique (IRRIT), Baseline and Alternative Cost Data, Engineering Estimates, and Assumptions"*

TABLE 17
FRC-SE EHC COST DATA.

Cost item	Quantity	Unit	Ann fixed	Unit	Ann Cost
EHC adoption					
Initial stripping & plating chemicals	$4,800	$			
Total adoption	$4,800	$			
EHC Summary costs					
Direct production labor	$265	$/sq ft			$47,190
Indirect production labor	$1.91	$/sq ft			$340
Direct materials	$26	$/sq ft			$4,690
Indirect materials	$0.46	$/sq ft			$82
Utilities	$86	$/sq ft			$15,385
Environmental	$560	$/sq ft			$99,611
Total	**$940**	**$/sq ft**			**$167,298**

EHC breakdown					
Water use: rinse + makeup			87,600	gal/yr	$209
Water use /sq ft	$1.18	$/sq ft	492	gal/sq ft	
Plating power /sq ft	$23.74	$/sq ft	323	kWh/sq ft	$4,226
Tank heater power (steam)	$61.52	$/sq ft	8,760	hr/yr	$10,950
Utilities total	**$86.43**	**$/sq ft**			
Scrubber energy cost	$280.90	$/sq ft	$50,000	$/yr	
Scrubber maintenance cost	$20.37	$/sq ft	$3,625	$/yr	
Stack testing, inspection	$44.83	$/sq ft	$7,980	$/yr	
NESHAP monitoring	$158.89	$/sq ft	432	hr/yr	$28,283
NESHAP reporting, training	$3.68	$/sq ft	10	hr/yr	$655
Haz waste management	$4.97	$/sq ft	13.5	hr/yr	$884
Haz waste disposal			6,500	lb/yr	$6,695
Haz waste disposal /sq ft	$37.61	$/sq ft	37	lb/sq ft	
Wastewater treatment			1,752	gal/yr	$1,489
Wastewater treatment /sq ft	$8.37	$/sq ft	10	gal/sq ft	
Environmental total	**$559.61**	**$/sq ft**	$99,611	$/yr	

TABLE 18
NCO-P COATING COSTS.

Cost item	Quantity	Unit	Ann fixed	Unit	Ann Cost
% workload replaced – ID EHC	19%				
Average ID part plated area	0.4	sq ft			
ID plating workload	34	sq ft			
Average ID plating process time	8.43	hr			
nCo-P Summary costs					
Direct production labor	$280	$/sq ft			$49,790
Indirect production labor	$2	$/sq ft			$358
Direct materials	$42	$/sq ft			$7,480
Indirect materials	$1	$/sq ft			$130
Utilities	$66	$/sq ft			$11,761
Environmental	$9	$/sq ft			$1,554
Total	**$399**	**$/sq ft**			**$71,073**

nCo-P breakdown					
Water use: rinse + makeup			262,800	gal/yr*	$628
Water use /sq ft	$3.53	$/sq ft	1,476	gal/sq ft	
Plating power /sq ft	$1.03	$/sq ft	14	kWh/sq ft	$183
Tank heater power (steam)	$61.52	$/sq ft	8,760	hr/yr	$10,950
Utilities total	**$66.07**	**$/sq ft**			
Scrubber energy cost	$0.00	$/sq ft	$0	$/yr	
Scrubber maintenance cost	$0.00	$/sq ft	$0	$/yr	
Stack testing, inspection	$0.00	$/sq ft	$0	$/yr	
NESHAP monitoring	$0.00	$/sq ft	0	hr/yr	$0
NESHAP reporting, training	$0.00	$/sq ft	0	hr/yr	$0
Haz waste management	$0.00	$/sq ft	0	hr/yr	$0
Haz waste disposal			2,167	lb/yr	$65
Haz waste disposal /sq ft	$0.37	$/sq ft	12	lb/sq ft	
Wastewater treatment			1,752	gal/yr	$1,489
Wastewater treatment /sq ft	$8.37	$/sq ft	10	gal/sq ft	
Environmental total	**$8.73**	**$/sq ft**	$1,554	$/yr	

* Estimate based on high bath temperature, with bath heated 24/7

Note: Depreciation not included in these costs

TABLE 19
NCO-P CAPITAL AND ADOPTION COSTS.

nCo-P capital cost	
Stripping tank, rectifier & wiring	$130,000
Maskant tank	$45,000
Activation tank, rectifier & wiring	$130,000
Plating rectifier & wiring*	$130,000
Carbon filtration equipment*	$6,000
Co anode tank*	$4,000
Total	**$445,000**
nCo-P adoption cost (initial chemicals)	
Stripping chemicals	$29,600
Maskant	$15,000
Plating chemicals	$18,100
Chemicals for anode tank	$3,000
Total	**$65,700**
Inflation rate	0%
Discount rate	3.00%
Depreciable life of equipment	15 yr
Salvage value	10%

* For modification of existing plating line

5.3 COST-BENEFIT ANALYSIS FOR FRC-SE

5.3.1 Capital cost

Capital cost (***Table 19***) depends on whether an existing line is to be modified or a new line is to be installed. In either case the pulse plating rectifier, carbon filtration and plating tank for anode production are required. But modifying an existing line avoids the requirement for additional tanks.

Note that we assume that the anode will typically be in the form of a plated rod rather than Co chips in a basket. This is because for many ID coating applications plated rod is the only viable approach, which requires the installation of a plating tank even if it is used for only some of the part production.

5.3.2 Direct manufacturing cost

Most of the labor cost of electroplating is involved with masking, demasking, setup, insertion and removal from the plating tank, and maintaining the plating system. The shorter plating cycle for CoP has little effect on the labor hours. Because the nCoP bath requires more maintenance for carbon filtration, and anode rods must be plated, the labor hours are somewhat higher for nCoP. In addition, the cost of chemicals is higher,

as is the cost of utilities because of the higher bath temperature, which requires more make-up water.

The direct cost of nCo-P vs hard chrome plating is summarized in ***Table 20***. The nCo-P direct cost is about slightly higher than hard chrome plating. However, when we add in the indirect costs and the environmental costs nCo-P costs $400/sq ft while hard chrome costs $940/sq ft (***Table 17 and Table 18)***. This is of course a very high unit cost, which comes about because, as shown in ***Table 16***, the plating volume is less than 200 sq ft/year, spreading all the fixed costs over a very small production volume. This unit cost would obviously be very much lower if the total workload were larger.

TABLE 20
DIRECT PRODUCTION COST PER SQUARE FOOT COMPARISON.

Cost per sq ft plated	nCo-P	EHC
Direct production labor	$280	$265
Direct materials	$42	$26
Utilities	$66	$86
	$388	**$377**

5.3.3 Cost-benefit for replacing full plating line

Table 21 shows the 15-year metrics for replacement of an entire line in an existing plating shop (which is equipped with all the necessary facilities, including heating and air handling). The cumulative cost for the relacement is shown as a function of time in ***Figure 12.***

TABLE 21
15–YEAR FINANCIAL PERFORMANCE FOR TOTAL LINE REPLACEMENT AT FRC-SE.

	-2 sigma	Value	+2 sigma
NPV	($53,711)	$222,830	$499,370
IRR	12%	15%	17%
ROI	13%	17%	21%
Payback period	13.7	8.5	5.9

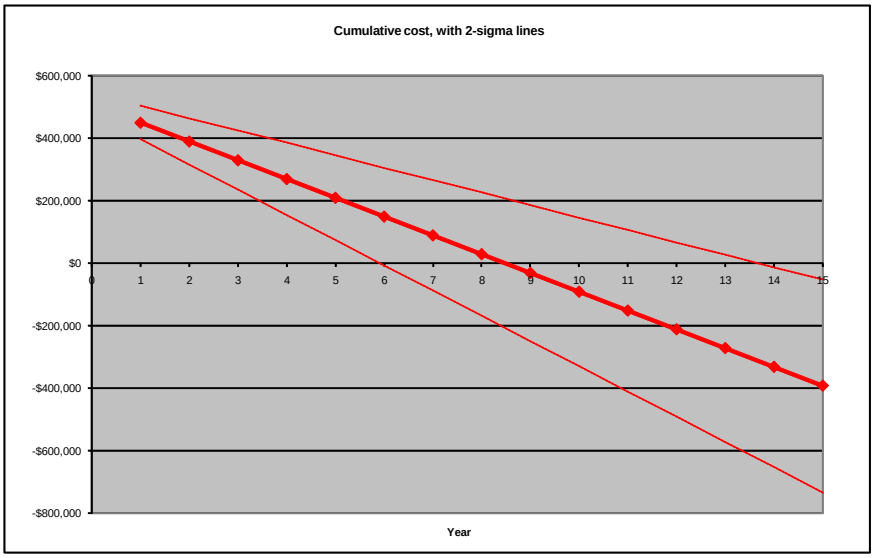

FIGURE 12. CUMULATIVE COST AS A FUNCTION OF TIME FOR TOTAL LINE REPLACEMENT AT FRC-SE (WITH 2σ LINES).

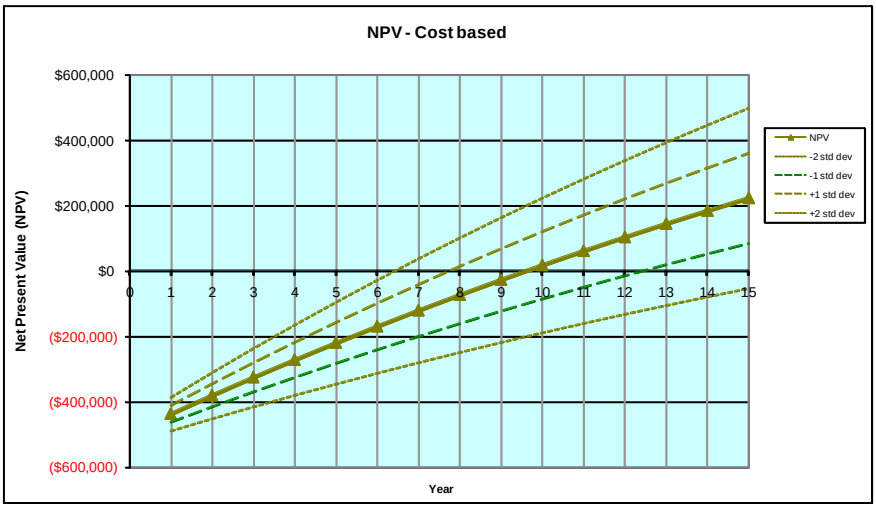

FIGURE 13. NPV AS A FUNCTION OF NUMBER OF YEARS INCLUDED IN ITS CALCULATION FOR TOTAL LINE REPLACEMENT AT FRC-SE (WITH 2σ LINES).

Note that in Table 21, the Internal Rate of Return and the Return on Investment are both annualized returns, not total returns, and they are based on the annual cost saving. For this reason the IRR and ROI can both be positive even when the NPV is negative, because the cumulative cost always slopes down. This is illustrated in the plot of Figure 13 which shows how NPV varies as a function of the number of years over which the NPV calculation is run. Note that NPV can still be negative even beyond the payback period, when cumulative cost has gone negative, because NPV discounts the value of money in the out years.

Although nCo-P is a more expensive process than hard chrome plating, and although it requires capital investment, it saves money because it eliminates the need for the Cr^{6+} scrubber, which costs more than $60,000 per year to maintain. What this means, however, is that adopting nCoP will only be cost-effective if it is used to completely eliminate hard chrome. If the scrubber is retained for other processes, or the chrome plating line is maintained, then savings will not be realized.

5.3.4 Cost-benefit for modifying existing plating line

In many cases nCoP will be implemented in an existing line. In this case only the items in ***Table 19*** that are marked with an asterisk will need to be purchased as capital equipment. In that case the NPV is significantly higher and the payback far faster because of the lower front-end cost of $140,000 instead of $445,000 (see ***Figure 14*** & ***Figure 15***).

TABLE 22
15–YEAR FINANCIAL PERFORMANCE FOR PLATING LINE MODIFICATION AT FRC-SE.

15 year	-2 sigma	Value	+2 sigma
NPV	$481,358	$737,410	$993,463
IRR	36%	42%	47%
ROI	31%	42%	53%
Payback period	3.7	2.6	2.0

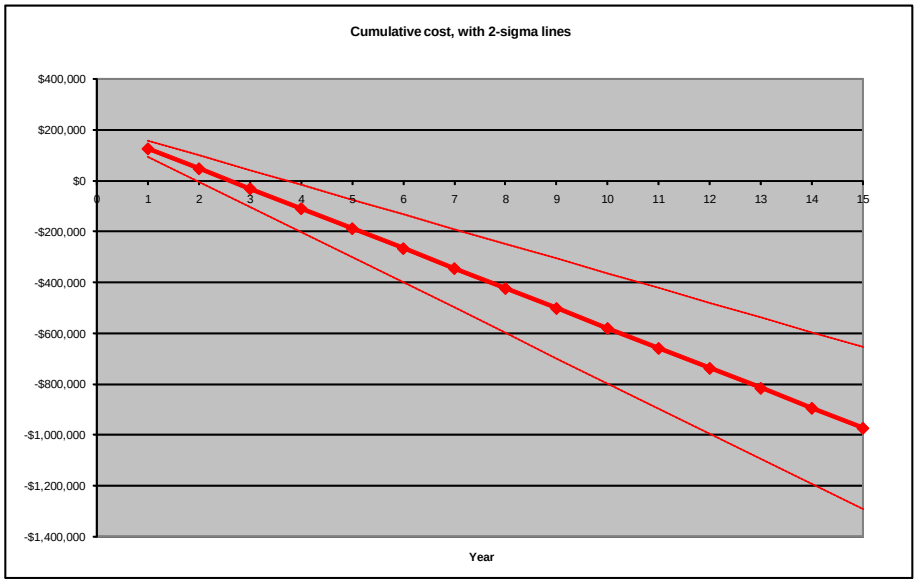

FIGURE 14. CUMULATIVE COST AS A FUNCTION OF TIME FOR PLATING LINE MODIFICATION AT FRC-SE (WITH 2σ LINES).

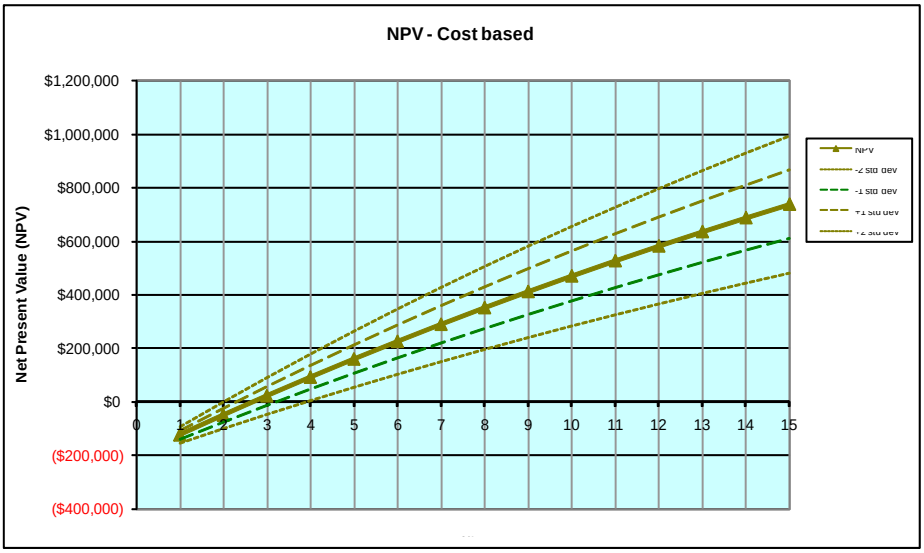

FIGURE 15. NPV AS A FUNCTION OF NUMBER OF YEARS INCLUDED IN ITS CALCULATION FOR PLATING LINE MODIFICATION AT FRC-SE (WITH 2σ LINES).

5.3.5 Effect of rework

Hard chrome plating is a very forgiving process that continues to plate even when tank chemistry or plating conditions are not optimum. It has been found that nCo-P, on the other hand, is much more sensitive to contamination in the bath, particularly in the form of hydrocarbons. Contamination causes holidays in the coating, necessitating stripping and replating. While contamination can be controlled through proper bath maintenance,

including carbon filtration and periodic dummying, we would expect that the incidence of rework would increase to some extent with the use of a more sensitive process.

Rework requires that the part be demasked, stripped, remasked and replated. The result of increased rework is illustrated in ***Figure 16*** assuming hard chrome rework is essentially zero, which is FRC-SE experience.

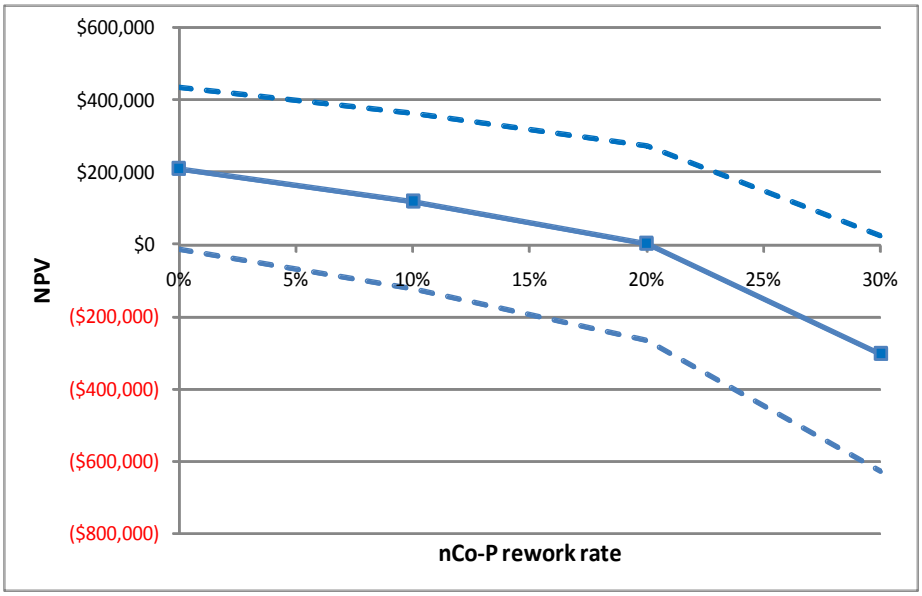

FIGURE 16. NPV AS A FUNCTION OF REWORK RATE (TOTAL PLATING LINE REPLACEMENT).

It is clear that, because it adds to production cost, rework reduces the payback from the technology. If rework increases to 20% the NPV drops to zero. It is therefore very important to maintain tank performance and ensure proper operator training in both tank maintenance and processing methods.

5.4 OPTIMUM METHOD OF ADOPTION

As we have seen, adoption of nCo-P will impose a net cost unless it completely replaces chrome plating. nCo-P plating will not begin to realize savings until the chrome scrubber is removed. If the changeover takes several years as components are tested and qualified then savings will not begin until chrome plating is completely eliminated and the scrubber shut down. Thus the optimum method of adoption is to qualify and move to production with the new coating as quickly as possible.

6.0 CONCLUSION

Optimized plating deposition parameters were obtained using a Design of Experiment (DOE) approach. These parameters were validated through supplemental testing and found to be non-embrittling with improved fatigue and neutral salt fog corrosion performance as compared to hard chromium electroplate. The nCoP deposit did exhibit reduced hardness (560 VHN) and reduced taber wear abrasion performance as compared to hard chromium electroplate.

Producibility evaluations were performed utilizing a J52 Shaft section and a J52 Coupling component. Optimized plating parameters were successfully demonstrated on both ID & OD areas. The above plated components were then finished machined at FRC-SE with no observable defects.

Final established and optimized parameters are:

- *Current Density:* 125 mA/cm^2
- *Frequency:* 25 Hz
- *Duty Cycle:* 50%

7.0 SUMMARY

nCo-P is an alternative electroplating process to EHC. The coating is very similar in appearance to EHC. The difference between this coating and standard cobalt-, nickel- or EHC-based coatings is the grain size of the deposit.

Nanocrystalline metals and alloys:
Electrodeposited nanocrystalline metals and alloys have an average grain size of roughly 5-15 nm. This is a reduction of about 1000 times that of the grain size of standard polycrystalline electrodeposited coatings. These nanocrystalline coatings have fully dense and equiaxed microstructures; as the coating is built up there is no grain growth or columnar growth. Typical properties that are improved by reducing the grain size to the nanocrystalline scale include:
Hardness: Up to 3-5X increase
Yield Strength: Up to 5-9X increase
Ultimate Tensile Strength: Up to 3-5X increase
Coefficient of Friction: Up to 50% reduction

nCo-P Process (***Table 23***): Like EHC, nCo-P is produced by electrodeposition. However, there are some key process differences as detailed below:
Anodes: Consumable cobalt anodes are used for the nCo-P process. These include cobalt pieces held in titanium baskets (OD plating and large ID plating), or cobalt-coated titanium rods (small ID plating). This is in contrast to EHC which uses non-consumable lead anodes.
Pretreatment: Like for EHC, recommended pretreatments vary with substrate material. Pretreatment steps are similar to EHC with one notable exception, in that activation does not take place in the plating tank. A separate process tank(s) is required for this step.
Masking: Wax-based maskants used for EHC cannot be used for the nCo-P process. Alternate dip and brush-on maskants are under investigation. Select electroplater's tapes can be used.
Efficiency and Plating Rate: The nCo-P process is significantly more efficient than EHC, thus resulting in much higher plating rates and increased process throughput.
Environmental: In contrast to EHC, air emissions from the nCo-P process do not contain harmful Cr^{6+}. Air emissions from the nCo-P process are below the OSHA PEL for cobalt. No scrubbers are required for the nCo-P process, however, local ventilation is suggested to remove steam from the area for worker comfort.
Hydrogen Embrittlement: Due to the high current efficiency, less hydrogen is generated for the nCo-P process compared to the EHC process. Nonetheless, hydrogen embrittlement relief bakeouts are currently recommended for high strength steels. This is similar to practices used for EHC.

Bath stability: The plating bath is very stable with only minor additions being required for pH balance and for the alloying compound. Since the anodes are consumable, no additions of cobalt salts are required.
Equipment: Similar electroplating equipment to EHC is required (i.e. tank, heater, pump, filter, buss bars, DI water supply, electrical connections to rectifier), however, the materials of construction must be compatible with the nCo-P plating bath. Unlike EHC, a pulse rectifier is required for the nCo-P process.

nCo-P Properties (*Table 24*): There are a number of key properties of the nCo-P that improves the performance when compared to EHC.
Appearance: The coating is similar in appearance to EHC.
Corrosion Protection: The coating has significantly improved corrosion protection over EHC, owing to the fully dense structure of the nCo-P coating.
Sliding Wear: The volume loss of material in sliding pin on disc wear tests is roughly one half that of EHC. Preliminary rod-seal wear testing suggests that nCoP has comparable seal leakage to EHC.
Lubricity: The coefficient of friction is approximately 20% less than EHC.
Abrasive wear: EHC does have higher abrasive wear performance. nCo-P may not be the most appropriate choice for EHC replacement in applications where abrasive wear mechanisms are known to operate. It is recommended that these be thoroughly reviewed and tested on a case-by-case basis.
Hardness: EHC has higher hardness. However, hardness does not necessarily correlate with sliding wear behavior, as evidenced by the improved sliding wear performance of nCo-P compared to EHC.
Fatigue: In early testing, nCo-P has shown significantly improved fatigue performance compared to EHC. In some cases, the nCo-P fatigue performance is comparable to the bare material.

TABLE 23 COMPARISON OF NCO-P AND EHC PROCESSES.

	nCo-P	**EHC**
Cathodic Current Efficiency	85-95%	15-35%
Deposition Rate	0.002”-0.008” per hour	0.0005”-0.001” per hour
Anodes	Consumable cobalt	Non-consumable lead
Hydrogen Embrittlement	Post-plate bakeout required	Post-plate bakeout required
Emission Analysis	Below OSHA limits	Cr^{+6}

TABLE 24 COMPARISON OF NCO-P AND EHC PROPERTIES.

Property	Test Method	Applicable Standard	nCo-P	EHC
Appearance and porosity	Visual and microscopic inspection	N/A	Free from pits, microcracks and pores	Microcracked
Grain Size	X-Ray Diffractometry	N/A	8-15 nm	-
Hardness	Vickers Microhardness	ASTM B578	550-600 VHN (as-deposited)	Min. 600 VHN
			600-750 VHN (heat treated)	-
Ductility	Bend Test	ASTM B489	2-7%	<1%
Adhesive Wear	Pin on Disc (Al_2O_3 Ball)	ASTM G99	6-7 x 10^{-6} mm^3/Nm	9-11 x 10^{-6} mm^3/Nm
Coefficient of friction	Pin on Disc (Al_2O_3 Ball)	ASTM G99	0.4-0.5	0.7
Pin Wear	Pin on Disc (Al_2O_3 Ball)	ASTM G99	Mild	Severe
Abrasive Wear	Taber Wear (CS-17 wheels)	ASTM D4060	17 mg/1000 cycles	4 mg/1000 cycles
Corrosion	Salt Spray	ASTM B117	0.003” thick Pass 165 h	0.003” thick Fail 165 h
			0.002” thick Protection Rating 7 (ASTM B537) @ 1000 hours	0.004” thick Protection Rating 2 (ASTM B537) @ 1000 hours
Deposit Stress	Internal Stress Test	N/A	10-15 ksi (Tensile)	Cracked – Exceeds cohesive strength
Fatigue	Rotating Beam Fatigue	N/A	Comparable to bare at high loads. Small debit compared to bare at low loads. Credit compared to EHC.	Significant debit compared to bare at all loads.

8.0 APPENDIX: ROD & SEAL TEST

8.1 HYDRAULIC SEAL AND PISTON ROD COATING EVALUATION OF NCOP

Rod and seal testing was performed in accordance with the HCAT Joint Test Protocol (JTP) to determine nCoP coating compatibility with common hydraulic and pneumatic seal materials. This JTP had been developed for testing HVOF coated rods (30 September 2003). The detailed test report is summarized in AIR 4.3.5 "Test Report For Hard Chrome Alternatives Team Phase III Hydraulic Seal and Piston Rod Coating Evaluation of Nanocrystalline-Cobalt-Phosphorus". Four rods were prepared at Fleet Readiness Center Southeast (FRC-SE) and sent to Integran Technologies Inc. for nCoP electroplating.

8.1.1 Test Summary

Different surface finish conditions were evaluated on each of the four rods as follows: (1) 12-16 min Ra, (2) 6-9 min Ra, (3) superfinished to <4 min Ra, and (4) heat treated at 300°C to maximize coating hardness, then ground to 6-9 min Ra. Each rod was tested against the same four seal configurations in the HVOF JTP: (1) MIL-P-83461 O-ring and PTFE cap strip, (2) MIL-P-83461 O-ring and 2 backup rings, (3) Fluorosilicone O-ring with PTFE cap strip, (4) Spring energized PTFE seal. As there were only four positions on the test equipment for different coatings/conditions, hard chrome controls were not run simultaneously.

8.1.2 Test Execution

The original test plan included fluid temperatures ranging from -40°F to 275°F, with ~80,000 sinusoidal full strokes superimposed with ~480,000 dither strokes. However, during testing, an incorrect computer stroke profile had been selected and run for the first five days of testing. At that time testing was stopped and the test sponsor authorized a revised test schedule to adjust the cycles to equate approximately to that originally planned. Hydraulic pressure ranged from between 2500-3000 psi.

8.1.3 Test Results – Leakage Rates

Leakage rates for all coating finishes are shown in ***Figure 17***. For comparison, EHC data from prior testing (not done in the same test as nCo-P) are also included. Leakage rates for all nCo-P coating finishes were acceptable for the duration of the test. Failure criterion is a leakage rate exceeding 1 drop for 25 full strokes, although this is different than the combination with the dither strokes. The superfinished nCo-P rod resulted in the least accumulated leakage over the test duration, followed by the heat treated rod, while the rougher ground finishes resulted in the highest leakage (6-9 and 12-16 min Ra finishes). For one seal configuration during 1 hour near the end of the test very slightly exceeded this rate (24.4 cycles per drop), however, this configuration leaks by design at cold temperatures so it wasn't considered significant.

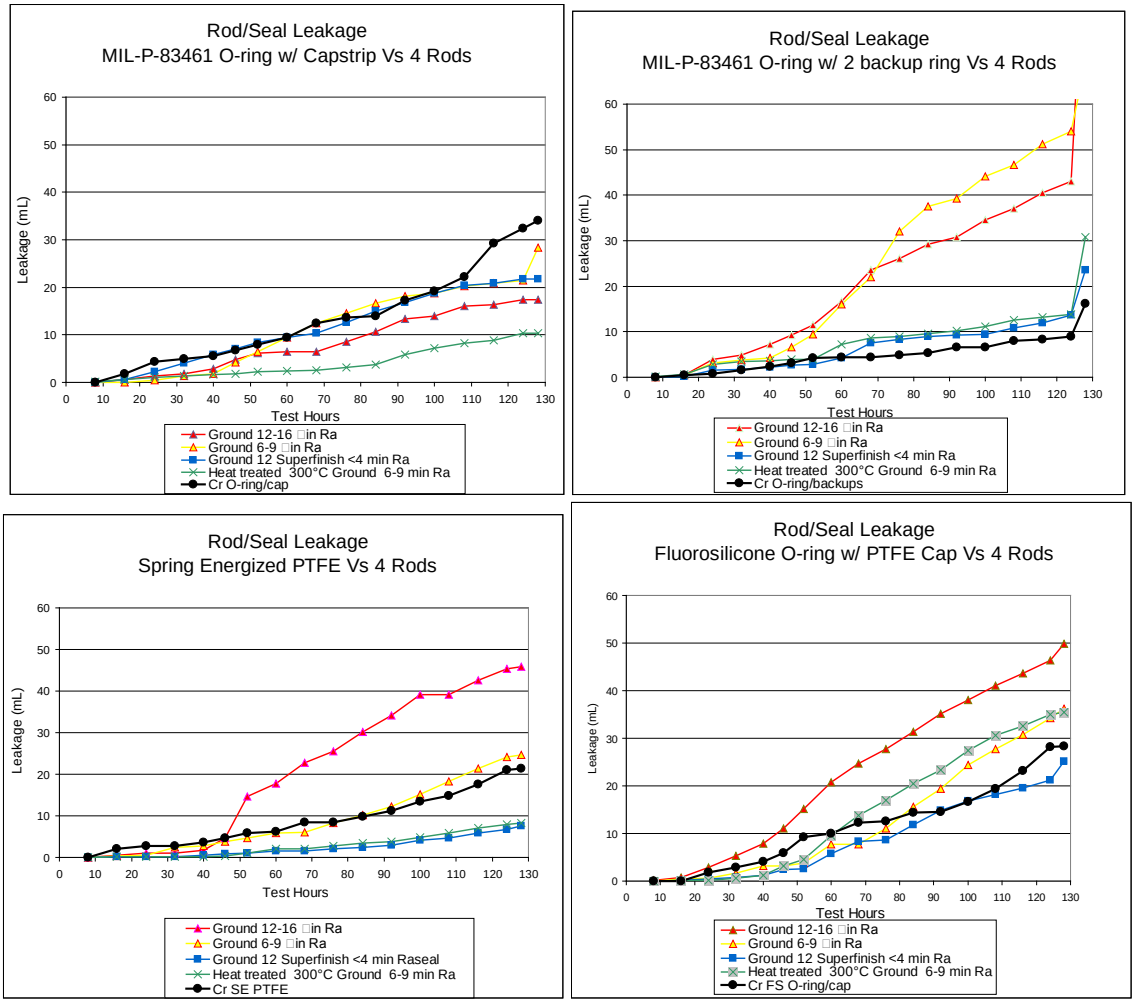

FIGURE 17. LEAKAGE RATES FOR NCO-P COATINGS WITH VARIOUS SURFACE FINISHES AND DIFFERENT SEAL CONFIGURATIONS. FOR REFERENCE, EHC DATA FROM PRIOR TESTS ARE INCLUDED.

8.1.4 Test Results – Seal Condition

At the conclusion of the test, rods and seals were removed from the test fixture, inspected and photographed, and then shipped to Supfina Inc. where seals were disassembled and inspected. Seal damage was noted for certain configurations. The AIR 4.3.5 test report concluded that the cap-strip seals failed due to excessive wear, and the seals with the most wear were noted on the rods with rougher finish. Seal images are available in the full report. Their recommendation was that a better simulation of flight conditions would incorporate a test under loaded conditions, including side loads.